

Dy-V magnetic interaction and local structure bias on the complex spin and orbital ordering in $\text{Dy}_{1-x}\text{Tb}_x\text{VO}_3$ ($x=0$ and 0.2)

J.-Q. Yan,^{1,2} H. B. Cao,³ M. A. McGuire,¹ Y. Ren,⁴ B. C. Sales,¹ and D. G. Mandrus^{1,2}

¹ *Materials Science and Technology Division, Oak Ridge National Laboratory, Oak Ridge, TN 37831, USA*

² *Department of Materials Science and Engineering,
University of Tennessee, Knoxville, TN 37996, USA*

³ *Quantum Condensed Matter Division, Oak Ridge National Laboratory, Oak Ridge, TN 37831, USA*

⁴ *X-ray Science Division, Argonne National Laboratory, Argonne, IL 60439, USA*

(Dated: June 9, 2022)

The spin and orbital ordering in $\text{Dy}_{1-x}\text{Tb}_x\text{VO}_3$ ($x=0$ and 0.2) was studied by measuring x-ray powder diffraction, magnetization, specific heat, and neutron single crystal diffraction. The results show that G-OO/C-AF and C-OO/G-AF phases coexist in $\text{Dy}_{0.8}\text{Tb}_{0.20}\text{VO}_3$ in the temperature range 2 K~60 K and the volume fraction of each phase is temperature and field dependent. The ordering of Dy moments at $T^*=12$ K induces a transition from G-OO/C-AF to a C-OO/G-AF phase. Magnetic fields suppress the long range order of Dy moments and thus the C-OO/G-AF phase below T^* . The polarized moments induced at the Dy sublattice by external magnetic fields couple to the V 3d moments and this coupling favors the G-OO/C-AF state. Also discussed is the effect of the Dy-V magnetic interaction and local structure distortion on the spin and orbital ordering in $\text{Dy}_{1-x}\text{Tb}_x\text{VO}_3$.

PACS numbers: 75.25.Dk, 75.40.-s, 61.66.Fn, 61.05.fm

INTRODUCTION

The orbital degree of freedom and its coupling with spin, charge and lattice in transition metal oxides have been interesting topics in condensed matter physics for many years.[1] The orbital physics of Jahn-Teller active e_g -electrons has been extensively studied in manganites where intriguing phenomena were observed due to strong electron correlations. In $R\text{VO}_3$ (R = rare earth and Y) perovskites, the octahedral-site V^{3+} ions with the electronic configuration of t^2e^0 have only π -bonding t_{2g} -electrons that are Jahn-Teller active. All $R\text{VO}_3$ members show a series of spin and orbital ordering transitions below room temperature.[2] Thus $R\text{VO}_3$ perovskites offer an ideal platform to study the orbital physics of π -bonding t_{2g} -electrons. A recent observation of ferroelectricity in DyVO_3 suggests that $R\text{VO}_3$ is a new family of magnetic multiferroics with strong coupling between electric polarization and spin/orbital ordered states.[3]

Two different types of orbital ordering were reported in $R\text{VO}_3$; in each the xy orbital is assumed to be occupied by one electron whereas the other electron takes yz and zx orbitals alternatively along $[100]$ and $[010]$ axes in the ab plane. The antiphase stacking of ab planes in G-type orbital order (G-OO, Fig. 1(a)) is in contrast to the in-phase stacking in C-type orbital order (C-OO, Fig. 1(b)).[4-6] The corresponding magnetic order, which is consistent with Goodenough-Kanamori rules,[7][8] is G-type (G-AF, Fig. 1(b)) for the C-OO state and C-type (C-AF, Fig. 1(a)) for G-OO state, respectively. $R\text{VO}_3$ members with $R=\text{La}, \dots, \text{Tb}$ have the G-OO/C-AF as the ground state. However, $R\text{VO}_3$ members with $R=\text{Dy}, \dots, \text{Lu}$ and Y show at low temperatures

a phase switch from G-OO/C-AF to C-OO/G-AF while cooling. Obviously, DyVO_3 is located near the boundary, and the delicate competition between the two distinct spin/orbital ordered states can be disturbed by external stimuli such as magnetic field or pressure.[9-12]

The complex spin and orbital ordering in DyVO_3 has been extensively studied by measuring the magnetic properties, thermal transport, structure, dielectric response, and optical properties.[9, 11] It's believed that 4 transitions take place in DyVO_3 : the G-type orbital order at $T_{OO}=190$ K, the C-type magnetic order at $T_N=113$ K, the transition from G-OO/C-AF to C-OO/G-AF at $T_{CG1}=57(\text{cooling})/64(\text{heating})$ K, and a re-entrant transition to G-OO/C-AF at $T_{CG2}=12(\text{cooling})/22(\text{heating})$ K. Strong hysteresis was found for the latter two transitions which are first order and accompanied by a structural transition between orthorhombic (Pbnm) for C-OO/G-AF and monoclinic ($\text{P}2_1/\text{b}$) for G-OO/C-AF. High pressure favors the C-OO/G-AF state which has a smaller volume.[9, 10] External magnetic fields applied along a - or b -axis favor the G-OO/C-AF state; in a magnetic field above 30 kOe, only the G-OO/C-AF state is observed below T_N . [11, 12] The picture that has emerged from several studies on $R\text{VO}_3$ ($R=\text{Dy}$, and Ho) suggests that both lattice distortions and Heisenberg magnetic exchange between the V 3d and R 4f moments need to be considered in order to understand the field-induced phase transitions.[12]

A recent single crystal neutron diffraction study provided direct evidence for a noncollinear, weak ferromagnetic order of the Dy sublattice below 12 K. The observed weak ferromagnetic order of the Dy sublattice suggests

an effective coupling of the external magnetic fields and the Dy sublattice. However, in sharp contrast to previous reports[9, 11] where G-OO/C-AF is believed to be the ground state for V-sublattice, this neutron diffraction study suggests that the ground state is C-OO/G-AF for the V-sublattice.

Besides the above discrepancy about the spin and orbital ordered ground state in DyVO_3 , how Dy^{3+} long range magnetic order responds to external magnetic fields is still unknown. In addition, a study on how small perturbation of the Dy sublattice affects the delicate balance between different spin and orbital ordered states is missing. Motivated by the above questions, we studied the spin and orbital ordering in $\text{Dy}_{1-x}\text{Tb}_x\text{VO}_3$ ($x=0$ and 0.2). The partial substitution of Dy by Tb is expected to disturb the long range order of Dy moments, and introduce local lattice distortion by the size difference between 12-oxygen coordinated Dy^{3+} and Tb^{3+} ions. Our results demonstrate that (1) Below 12 K, the long range magnetic order of Dy^{3+} moments in DyVO_3 favors the C-OO/G-AF phase for the V-sublattice, which introduces a small fraction of C-OO/G-AF phase in the dominant G-OO/C-AF matrix; (2) external magnetic fields suppress the long range order of Dy^{3+} moments thus destabilizing the C-OO/G-AF phase in the Dy ordered state; (3) the polarized Dy^{3+} moments favor the G-OO/C-AF phase. In addition, we find that partial substitution of Dy by Tb induces phase coexistence of G-OO/C-AF and C-OO/G-AF in a wide temperature range below T_{CG1} ; the fraction of each phase is temperature and field dependent. The effects of Dy-V magnetic interactions and local structural distortions on the spin and orbital ordering are discussed.

EXPERIMENTAL DETAILS

DyVO_3 and $\text{Dy}_{0.8}\text{Tb}_{0.2}\text{VO}_3$ single crystals were grown with the floating zone technique. [14] A DyVO_3 single crystal grown in a similar manner was investigated in a previous study.[9] Elemental analysis of the crystals was performed using a Hitachi TM-3000 tabletop electron microscope equipped with a Bruker Quantax 70 energy dispersive X-ray (EDX) system. The analysis confirmed that the as-grown crystal has the nominal stoichiometry within experimental error. X-ray powder diffraction on pulverized single crystals was performed using a PANalytical X'Pert Pro MPD powder X-ray diffractometer with a copper target in the temperature range $16\text{ K} \leq T \leq 300\text{ K}$. Close inspection of the powder diffraction patterns at room temperature revealed no impurity phases. For $\text{Dy}_{0.8}\text{Tb}_{0.2}\text{VO}_3$, all observed reflections could be indexed using the orthorhombic space group (Pbnm) with lattice parameters of $a = 5.305(1)\text{ \AA}$, $b = 5.607(2)\text{ \AA}$, and $c = 7.599(2)\text{ \AA}$. The high-energy high-resolution X-ray powder diffraction was performed at 11ID-C, Advanced Photon Source, Argonne National

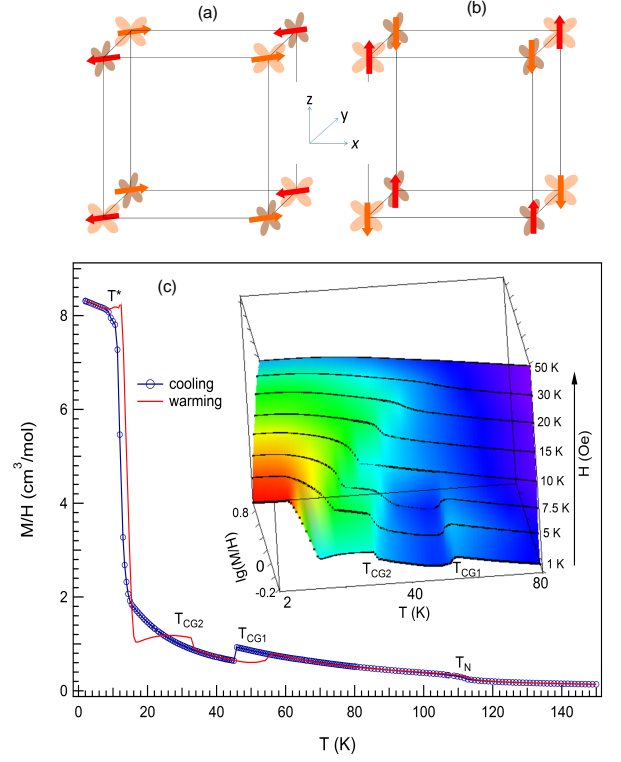


FIG. 1: (Color online) (a) Schematic diagram of the G-type orbital order (G-OO) with the C-type magnetic order (C-AF). (b) Schematic diagram of the C-type orbital order (C-OO) with the G-type magnetic order (G-AF). (c) The temperature dependence of M/H of $\text{Dy}_{0.8}\text{Tb}_{0.2}\text{VO}_3$ measured upon cooling and warming in a magnetic field of 1 kOe. The inset shows the magnetization curves measured in various magnetic fields upon warming.

Laboratory. Single crystal neutron diffraction was measured at HB-3A four-circle diffractometer at the High Flux Isotope Reactor at the Oak Ridge National Laboratory. A neutron wavelength of 1.003 \AA was used with a bent perfect Si-331 monochromator.[15] Magnetic properties were measured with a Quantum Design (QD) Magnetic Properties Measurement System in the temperature interval $2.0\text{ K} \leq T \leq 300\text{ K}$. The temperature dependent specific heat data were collected using a 9 Tesla QD Physical Properties Measurement System in the temperature range of $1.9\text{ K} \leq T \leq 300\text{ K}$.

EXPERIMENTAL RESULTS

Figure 1(c) shows the temperature dependence of the M/H of $\text{Dy}_{0.8}\text{Tb}_{0.2}\text{VO}_3$ in an applied magnetic field of 1 kOe measured both cooling and warming. The orientation of the sample is not well defined since Laue diffraction shows the crystal contains a few grains which prevents the study of anisotropic magnetic properties. The crystal was first cooled to 2 K in zero magnetic field.

At 2 K, a magnetic field of 1 kOe was applied and the magnetization was measured while warming to 300 K. Then the magnetization data were collected while cooling from 300 K to 2 K. The rare earth moments dominate the paramagnetic state and no slope change was observed around T_{OO} in the temperature dependence of H/M (not shown) for $Dy_{0.8}Tb_{0.2}VO_3$. For RVO_3 members with nonmagnetic rare earth ions ($R = Y, Lu, Y_{1-x}La_x$), a slope change in H/M is normally observed at T_{OO} . [16–18] As shown later in the temperature dependence of specific heat, T_{OO} was determined to be 195 K for $Dy_{0.8}Tb_{0.2}VO_3$. Below T_{OO} , the magnetization curve clearly shows multiple magnetic orderings. An increase of magnetization at 113 K suggests the onset of long range magnetic order of the V-sublattice at $T_N = 113$ K. The increase of magnetization is due to a weak spin canting resulting from the Dzyaloshinsky-Moriya antisymmetric exchange interaction in the G-OO/C-AF phase. No hysteresis was observed around T_N which agrees with the second-order nature of this transition. Below T_N , two step-like anomalies at $T_{CG1} = 46$ K and $T^* = 12$ K were observed with decreasing temperature; however, three could be well resolved at $T^* = 14$ K, $T_{CG2} = 33$ K and $T_{CG1} = 56$ K with increasing temperature. The absence of T_{CG2} in the cooling process is similar to that in $DyVO_3$. Compared to $DyVO_3$, $Dy_{0.8}Tb_{0.2}VO_3$ shows similar T^* , T_N , and T_{OO} , but T_{CG2} takes place at a higher temperature and T_{CG1} occurs at a lower temperature. This suggests that the transition between C-OO/G-AF and G-OO/C-AF states at T_{CG1} and T_{CG2} is more sensitive to the rare earth site substitution. The step-like change and large hysteresis of magnetization at T_{CG1} and T_{CG2} agrees with the first-order nature of these two transitions. A small hysteresis at T^* signals that the transition at T^* is different from a simple regular second-order magnetic transition involving only the Dy sublattice.

The inset of Fig.1(c) shows the M/H data of $Dy_{0.8}Tb_{0.2}VO_3$ measured upon warming in various magnetic fields. No field dependence of T_N was observed in this study. The sharp change of M/H at T^* broadens, decreases in magnitude, and shifts to higher temperatures with increasing magnetic fields. As this anomaly meets T_{CG2} at $H \geq 10$ kOe, the step-like change at T_{CG1} and T_{CG2} disappears. It's worth mentioning that the field dependence for T_{CG1} and T_{CG2} is small before they disappear. This is in contrast to a large field dependence of T_{CG2} in $DyVO_3$. [11]

Figure 2 shows the field dependence of magnetization measured at various temperatures. The jump in magnetization at low temperatures signals the occurrence of a metamagnetic transition. At 2 K, a saturation moment of about $7.8 \mu_B$ per formula unit was observed. Compared with the $M(H)$ curves of $DyVO_3$, [11] the data in Fig. 2 suggest that (1) the measurement is performed mainly along crystallographic b-axis, and (2) the metamagnetic transition is related to the rare earth 4f moments since a

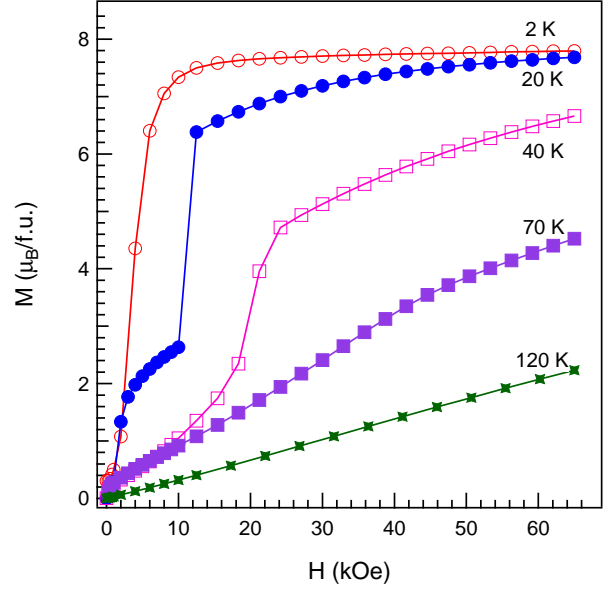


FIG. 2: (Color online) Field dependence of magnetization of $Dy_{0.8}Tb_{0.2}VO_3$ measured at indicated temperatures.

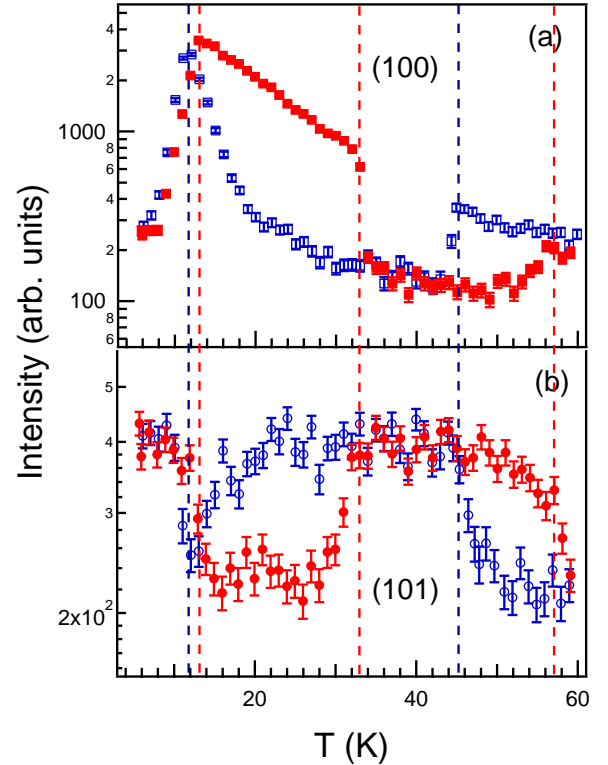


FIG. 3: (Color online) The temperature dependence of intensity of (100) and (101) magnetic reflections of $Dy_{0.8}Tb_{0.2}VO_3$ measured both warming (solid symbols) and cooling (open symbols). The vertical dashed lines highlight the temperatures where the intensity of (100) and (101) changes. The magnetic order of V sublattice in G-AF and C-AF ordered states could be distinguished by the (101) and (100) reflections, respectively.

maximum magnetic moment of $2\mu_B$ is expected for V^{3+} .

To confirm the magnetic orderings suggested by the $M(T)$ data shown in Fig. 1(c), single crystal neutron diffraction was performed in the temperature interval $4\text{ K} \leq T \leq 60\text{ K}$ in zero magnetic field. From previous measurements,[13, 19] the magnetic order of the V sublattice in G-AF and C-AF ordered states could be distinguished by the (101) and (100) (in orthorhombic notation) magnetic reflections, respectively. Figure 3 shows the temperature dependence of intensity of (100) and (101) magnetic reflections measured upon both heating and cooling. As shown in Fig. 3(a), with increasing temperature, the intensity of (100) shows a sharp increase around 12 K, then decreases slowly until 33 K where a step-like drop takes place. At approximately 56 K, the intensity of (100) shows another quick increase and reaches almost the same intensity as observed around 5 K. When measured while cooling, the intensity of the (100) peak shows a step-like drop at 46 K, then a gradual increase until $\sim 20\text{ K}$ below which the intensity increases quickly to a maximum around 11 K. Below 11 K, the intensity quickly drops to a value similar to that observed at $\sim 60\text{ K}$. In contrast, the intensity of (101) magnetic reflection shows an opposite temperature dependence. With increasing temperature, the intensity shows a quick drop around 12 K and a rapid increase around 32 K, respectively. Above 30 K it shows a sharp increase to a value similar to that below 10 K, and then drops to be similar to that at 20 K above 58 K. During cooling, the intensity increases below 48 K and shows a dip around 12 K.

To confirm that Dy^{3+} moments order at low temperatures, the temperature dependence of the (200), (002), and (202) reflections was monitored in the temperature range $4\text{ K} \leq T \leq 60\text{ K}$ during both warming and cooling. These reflections are structurally allowed and an intensity change is expected at T^* . [13] The results plotted in Fig. 4 clearly show that Dy moments order below 12 K and a small ($\sim 2\text{ K}$) hysteresis agrees with the observation in magnetization measurements shown in Fig. 1(c). The observed hysteresis is unusual since the Dy moment ordering is expected to be a continuous transition. This unusual feature is similar to that observed in $DyVO_3$ [13] and suggests that the long range magnetic order of Dy^{3+} moments is accompanied with a transition between G-OO/C-AF and C-OO/G-AF states. Above T^* , the peak intensity shows little difference when measured during cooling and warming. In contrast, in the temperature interval $12\text{ K} \leq T \leq 22\text{ K}$, (002) and (202) reflections of $DyVO_3$ are stronger in intensity when measured on warming than on cooling. The neutron single crystal diffraction study on $DyVO_3$ suggests a $(C_x, F_y, -)$ and $(F_x, C_y, -)$ type magnetic order of Dy^{3+} moments below and above T^* , respectively. [13] The results shown in Fig. 4 suggests that partial substitution of Dy by Tb disturbs the ordering of Dy^{3+} moments above T^* .

The temperature dependence of the intensity of

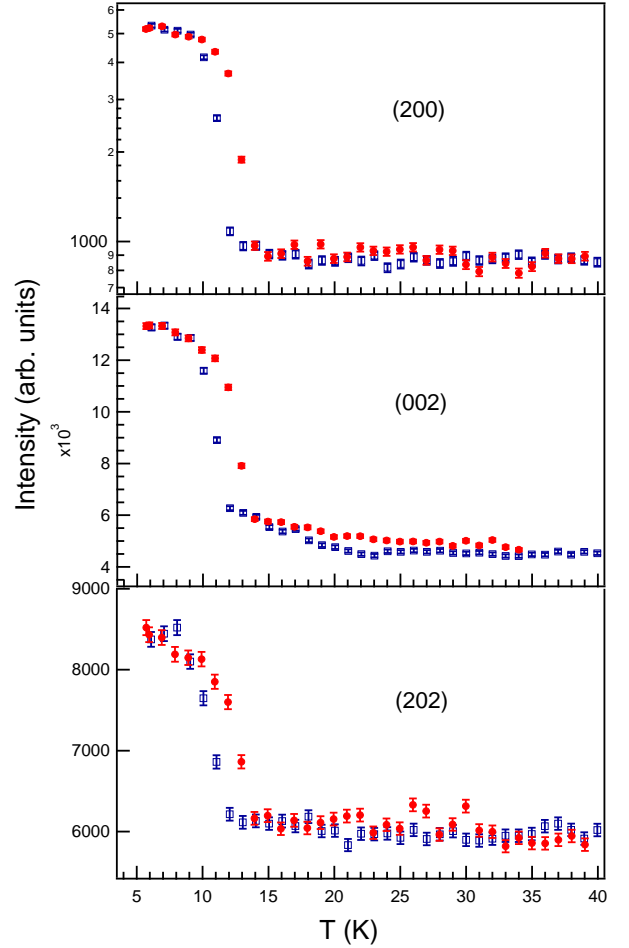


FIG. 4: (Color online) The temperature dependence of intensity of (200), (002) and (202) reflections of $Dy_{0.8}Tb_{0.2}VO_3$ measured upon both warming (solid symbols) and cooling (open symbols).

the above studied magnetic reflections confirms in $Dy_{0.8}Tb_{0.2}VO_3$: (1) the long range magnetic order of Dy moments and the observation of C-OO/G-AF phase below T^* ; (2) on warming, the G-OO/C-AF state was observed in the temperature range $12\text{ K} \leq T \leq 32\text{ K}$, while the C-OO/G-AF state was favored for $32\text{ K} \leq T \leq 58\text{ K}$; (3) with decreasing temperature, the C-OO/G-AF state was observed in a wider temperature range below 42 K. The above features are similar to those in $DyVO_3$. [13] However, the dip in the temperature dependence of the (101) peak around T^* (see Fig. 3(b)) is absent in $DyVO_3$. The gradual change of the intensity of the (100) and (101) reflections below $\sim 20\text{ K}$ suggests both the coexistence of G-OO/C-AF and C-OO/G-AF phases near T^* and that the fraction of each phase is temperature dependent.

The transition from G-OO/C-AF to C-OO/G-AF is accompanied by a volume contraction. [4] To confirm the structural transitions and determine the phases in different temperature intervals, X-ray powder diffraction

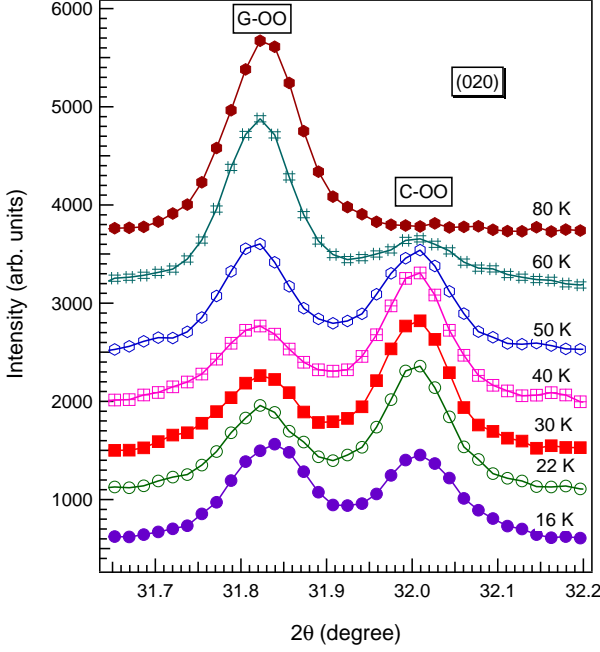


FIG. 5: (Color online) X-ray powder diffraction patterns of $\text{Dy}_{0.8}\text{Tb}_{0.2}\text{VO}_3$ measured using a PANalytical X'Pert Pro MPD powder X-ray diffractometer with copper anode. The patterns were shifted vertically for clarity.

experiments were performed. Uniform powder pulverized from single crystals was first cooled down to 80 K. Powder diffraction data were collected over a 2θ range of $10^\circ \leq 2\theta \leq 70^\circ$ for selected temperatures from 80 K to the base temperature at 16 K. Figure 5 shows the temperature dependence of the $(020)_{\text{orth}}$ peak measured in the temperature range $16 \text{ K} \leq T \leq 80 \text{ K}$ to highlight the phase evolution with temperature for $\text{Dy}_{0.8}\text{Tb}_{0.2}\text{VO}_3$. At 80 K in the G-OO/C-AF state, a single peak at $2\theta = 31.84^\circ$ was observed. At 60 K, the peak at $2\theta = 31.84^\circ$ drops in intensity and one new peak appears at $2\theta = 32.01^\circ$ signaling the appearance of the C-OO/G-AF phase. Below 60 K, the coexistence of both G-OO/C-AF and C-OO/G-AF phases was well resolved with X-ray powder diffraction. The volume fraction (roughly estimated from the peak intensity) of the C-OO/G-AF phase increases below 60 K and then decreases below $\sim 30 \text{ K}$. Our X-ray diffraction system was not able to measure below T^* . To confirm the phase coexistence below T^* , synchrotron X-ray powder diffraction was performed at 5 K after cooling from room temperature (See Fig. 6(a)). The double-peak feature agrees with the phase-coexistence scenario. The disappearance of the peak at $2\theta = 4.49^\circ$ in a field of 65 kOe signals that a large magnetic field can destroy the C-OO/G-AF phase. For comparison, Fig. 6(b) shows the diffraction patterns of $(040)_{\text{orth}}$ peak for DyVO_3 collected at different temperatures. At 5 K, a weak, broad peak at $2\theta = 4.49^\circ$ signals the existence of small amount of

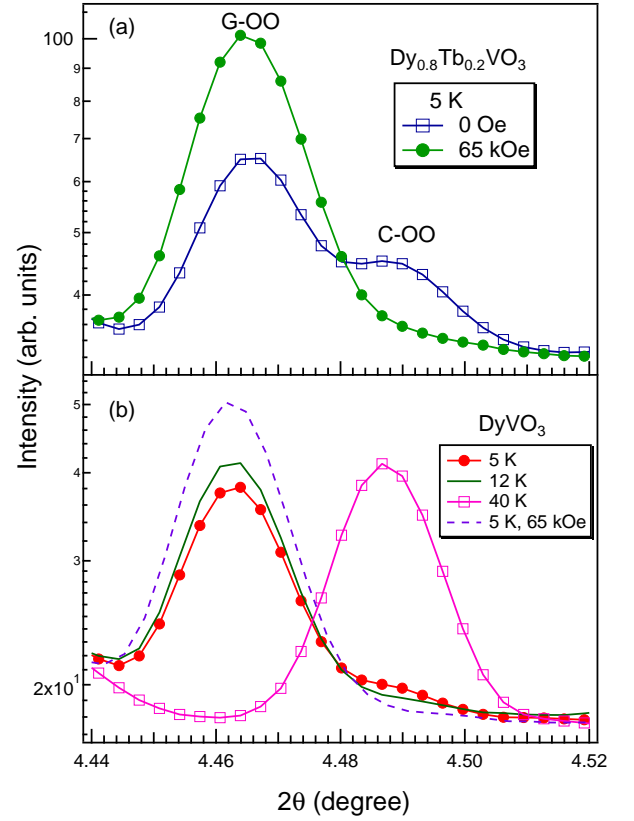


FIG. 6: (Color online) Evolution of $(040)_{\text{orth}}$ peak with temperature and magnetic field for (a) $\text{Dy}_{0.8}\text{Tb}_{0.2}\text{VO}_3$ and (b) DyVO_3 . The high-energy high-resolution powder diffraction experiment was performed using a wavelength of $\lambda = 0.108 \text{ \AA}$.

C-OO/G-AF phase together with the majority G-OO/C-AF phase. The volume fraction of the C-OO/G-AF phase estimated from the peak intensity is much less than that in $\text{Dy}_{0.8}\text{Tb}_{0.2}\text{VO}_3$. With increasing temperature, this peak decreases in intensity and is barely observable at $\sim 12 \text{ K}$; above T_{CG2} it becomes dominant signaling the transition from the G-OO/C-AF state to the G-OO/C-AF state. As in $\text{Dy}_{0.8}\text{Tb}_{0.2}\text{VO}_3$, a large magnetic field wipes off the minority C-OO/G-AF phase at 5 K. In contrast, the phase coexistence in DyVO_3 was only observed in the Dy ordered state below 12 K. This clearly suggests that long range magnetic order of Dy moments favors the C-OO/G-AF state. We note that the G-OO/C-AF phase dominates below T^* in DyVO_3 . The small fraction of C-OO/G-AF phase is not stable under applied magnetic fields. The disappearance of the minor C-OO/G-AF phase below T^* under applied magnetic fields in turn suggests that the long range order of Dy moments is suppressed by applied magnetic fields.

In order to further explore the magnetic field effect on the magnetic order of Dy moments, the specific heat of DyVO_3 was measured in 0 Oe and 10 kOe, respectively. As shown in Fig. 7 which plots C_p/T vs T , in zero field a

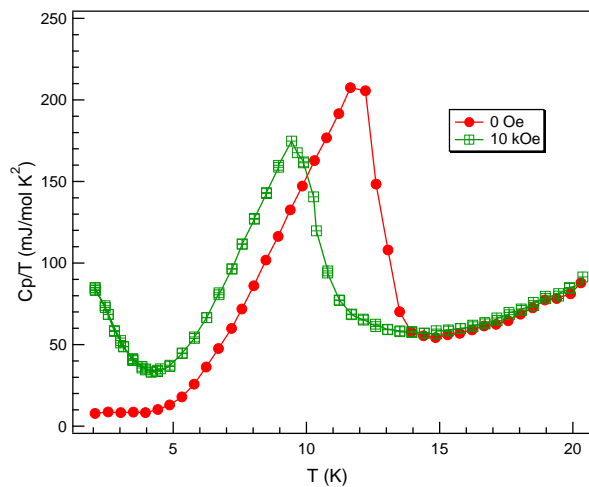


FIG. 7: (Color online) Magnetic field effect on the temperature dependence of specific heat of DyVO_3 near 12 K.

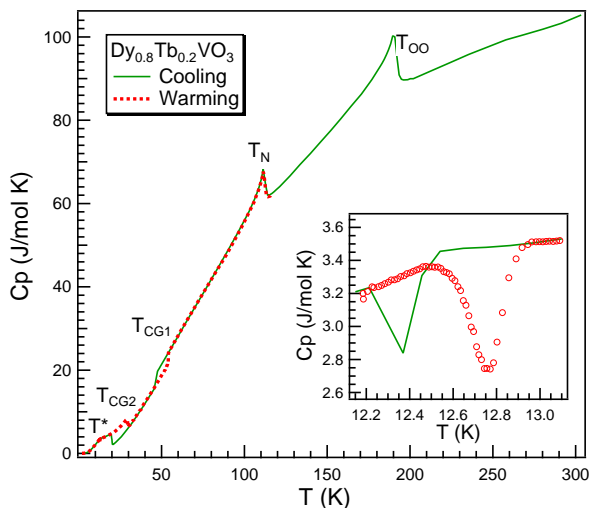


FIG. 8: (Color online) The temperature dependence of specific heat of $\text{Dy}_{0.8}\text{Tb}_{0.2}\text{VO}_3$. Inset highlights the details around 12 K.

lambda-type anomaly is well resolved at 12 K (peak position) where Dy^{3+} moments order. Once an external magnetic field of 10 kOe is applied, the lambda-type anomaly shifts to about 9 K and a Schottky-anomaly-like feature appears below 4 K. The results clearly illustrate that external magnetic fields suppress the long range magnetic order of Dy moments. Measurements at even larger magnetic fields failed because the Apiezon N-grease failed to hold the sample on the stage due to the large torque that the sample experienced.

Figure 8 shows the temperature dependence of specific heat of $\text{Dy}_{0.8}\text{Tb}_{0.2}\text{VO}_3$ measured in the temperature range $1.9 \text{ K} \leq T \leq 300 \text{ K}$. Two lambda-type anomalies could be well resolved at $T_{OO}=195 \text{ K}$ and $T_N=113 \text{ K}$,

respectively. No hysteresis was observed at T_N , which agrees with the magnetization measurement. When measured on warming, T_{CG1} and T_{CG2} determined from the step-like change agree with those obtained by magnetization and neutron measurements. With decreasing temperature, T_{CG1} is lowered to 46 K, and another step-like change was observed at 20 K signaling the transition from C-OO/G-AF to G-OO/C-AF. We noticed that on cooling the intensity of the (100) peak shows a sharper increase while the intensity of the (101) peak starts to decrease below 20 K, although no obvious anomaly was observed in the M/H curve in Fig. 1. These results suggest that $T_{CG2}=20 \text{ K}$ on cooling. Around T^* , $\text{Cp}(T)$ shows a weak lambda-type anomaly. The inset of Fig. 8 shows the details of $\text{Cp}(T)$ around T^* . Surprisingly, a dip on top of the broad lambda-type anomaly was observed in $\text{Cp}(T)$ curve while both cooling and warming with a hysteresis of approximately 0.4 K. This feature is unusual in the temperature dependence of specific heat. Considering that a lambda-type anomaly is expected for the continuous magnetic order of Dy moments and a step-like decrease of $\text{Cp}(T)$ takes place at the transition from G-OO/C-AF to C-OO/G-AF, the unusual dip in $\text{Cp}(T)$ curve suggests that a transition from G-OO/C-AF to C-OO/G-AF happens accompanying the magnetic ordering of Dy moments when cooling across T^* . A detailed measurement of $\text{Cp}(T)$ of DyVO_3 around T^* failed to observe the dip-like feature as shown in the inset of Fig. 8. This is as expected because $\text{Cp}(T)$ around T^* is dominated by the well resolved lambda-type anomaly and also the volume fraction of the G-OO/C-AF phase that changes to C-OO/G-AF is small consistent with the X-ray powder diffraction data shown in Fig. 6.

DISCUSSION

In both $\text{Dy}_{0.8}\text{Tb}_{0.2}\text{VO}_3$ and DyVO_3 , our study observed long range magnetic order of Dy moments and the coexistence of C-OO/G-AF and G-OO/C-AF phases below T^* . Also, a series of spin and orbital ordering transitions take place above T^* with increasing temperature at T_{CG1} , T_{CG2} , T_N , and T_{OO} , respectively. However, partial substitution of Dy by Tb induces the following differences between $\text{Dy}_{0.8}\text{Tb}_{0.2}\text{VO}_3$ and DyVO_3 that are noteworthy:

(1) In DyVO_3 , the phase coexistence was observed only when Dy moments order below $T^*=12 \text{ K}$. However, the coexistence of G-OO/C-AF and C-OO/G-AF phases was observed in a wide temperature interval below $T_{CG1}=58 \text{ K}$ in $\text{Dy}_{0.8}\text{Tb}_{0.2}\text{VO}_3$. The volume fraction of each phase is temperature and field dependent.

(2) Tb substitution lowers T_{CG1} but increases T_{CG2} which means that the C-OO/G-AF phase is destabilized. T_{CG2} could be resolved in $\text{Cp}(T)$ data when measured during both heating and cooling. With decreasing tem-

peratures, the anomalies in the intensities of (100), (101), and (002) reflections took place at about 20 K where a step-like jump was observed in $C_p(T)$ data.

(3) A large field dependence of T_{CG2} was reported in $DyVO_3$. [11] In contrast, T_{CG2} of $Dy_{0.8}Tb_{0.2}VO_3$ shows little field dependence before it disappears when the external magnetic field is larger than 10 kOe.

(4) A well-resolved lambda-type anomaly at T^* in the $C_p(T)$ curve of $DyVO_3$ was replaced by a weak anomaly in $Dy_{0.8}Tb_{0.2}VO_3$. The reduced entropy change across T^* makes it possible to observe the specific heat change due to the phase transition from G-OO/C-AF to C-OO/G-AF driven by the ordering of Dy moments.

In RVO_3 perovskites, the rare earth ions stay in the center of the dodecahedron formed by oxygen. The $GdFeO_3$ -type distortion which involves the cooperative octahedral-site rotations is proportional to the ionic radius of the rare earth ions and affects the spin and orbital ordering of the V-sublattice. [20, 21] Partial substitution of Dy by Tb (1) increases the average ionic radius of the rare earth site, (2) introduces rare earth site variance due to the ionic radius difference between Dy^{3+} and Tb^{3+} . The effect of size variance on the spin and orbital ordering in RVO_3 perovskites has been studied in $Y_{1-x}La_xVO_3$, [18, 19] $Y_{1-x}(La_{0.23}Lu_{0.77})_xVO_3$, [19] $Y_{1-x}Eu_xVO_3$, [12] and $Eu_{1-x}(La_{0.254}Y_{0.746})_xVO_3$. [22] Despite a different understanding of how quenched disorder affects the spin and orbital ordering, both Yan *et al.* [18, 19] and Fukuta *et al.* [22] observed that the rare earth size variance suppresses T_{OO} and T_N but enhances T_{CG} . By contrast, the study of $Y_{1-x}Eu_xVO_3$ by Fujioka *et al.* [12] showed that G-OO/C-AF phase is stabilized and C-OO/G-AF phase is destabilized with increasing x . The substitution effect of Dy by Tb observed in this study is similar to that in $Y_{1-x}Eu_xVO_3$. Obviously, there are two distinct effects of quenched disorder on the spin and orbital ordering in RVO_3 perovskites.

In all compositions mentioned above which show suppressed T_{OO} and T_N and enhanced T_{CG} by quenched disorder, nonmagnetic La^{3+} ions are present at the rare earth site. To rule out the possibility that this suppression is due to the nonmagnetic feature of La^{3+} ions, we also studied the substitution effect of Y by Nd in YVO_3 . Our preliminary study on the spin and orbital ordering in $Y_{1-x}Nd_xVO_3$ suggests that Nd substitution suppresses T_{OO} and T_N , but enhances T_{CG} ; 20% Nd increases T_{CG} to 85 K as does 5% La in $Y_{1-x}La_xVO_3$. These results strongly suggest that there is a critical local stress field above which the G-OO/C-AF phase is destabilized while the C-OO/G-AF phase is more stable. The partial substitution of Y by Eu in $Y_{1-x}Eu_xVO_3$ or Dy by Tb in $Dy_{1-x}Tb_xVO_3$ does increase the average ionic radius of rare earth site and induce size variance. However, the local stress field generated by the substitutional rare earth ions is below the critical value. Thus T_{CG} is suppressed by the rare earth site disorder. The enhanced T_{OO} and

T_N in $Y_{1-x}Eu_xVO_3$ suggests that T_{OO} and T_N mainly depend on the average structure, i.e., the increased V-O-V bond angle. Therefore, in considering the effect of quenched disorder on the spin and orbital ordering in RVO_3 perovskites, the magnitude of the local stress field generated by a single foreign atom is another factor in addition to the average ionic radius and size variance.

Despite suppressing T_{CG1} , the partial substitution of Dy by Tb favors the phase coexistence of C-OO/G-AF and G-OO/C-AF states below $T_{CG1} = 56$ K as revealed by X-ray powder diffraction patterns shown in Fig. 5 and 6. This is in sharp contrast to $DyVO_3$ where the phase coexistence was observed only in the Dy^{3+} ordered states below 12 K. As discussed later, the long range magnetic order of Dy^{3+} moments favors the C-OO/G-AF phase and introduces a phase transition from G-OO/C-AF to C-OO/G-AF. However, the disturbed Dy-V magnetic interaction by Tb substitution cannot explain (1) the phase coexistence in $Dy_{0.8}Tb_{0.2}VO_3$ in the temperature range below $T \leq T_{CG2}$, or (2) more of the C-OO/G-AF phase in $Dy_{0.8}Tb_{0.2}VO_3$ below T^* than for $DyVO_3$ since the long range order of Dy^{3+} moments favor the C-OO/G-AF phase. We thus have to attribute the phase coexistence in a wide temperature range below T_{CG1} to the local structure effect induced by Tb substitution. The phase coexistence further highlights the importance of local structure distortion in stabilizing the spin and orbital ordered states in $DyVO_3$ and agrees with the fact that the delicate balance between C-OO/G-AF and G-OO/C-AF states can be tuned with a small external stimulus. The evolution of the volume fraction of each phase with temperature suggests a temperature dependent change of the local structural distortion.

The long range order of Dy^{3+} moments affects the spin and orbital ordering of the V-sublattice. In addition, strong external magnetic fields destroy the C-OO/G-AF phase. Two observations in this study suggest that the ordered Dy^{3+} moments below $T^* = 12$ K prefer the C-OO/G-AF state. First, synchrotron X-ray powder diffraction measurements reveal a small amount of the C-OO/G-AF phase in $DyVO_3$ below T^* , which gradually disappears while warming above T^* . Second, the dip-like feature in the temperature dependence of the specific heat of $Dy_{0.8}Tb_{0.2}VO_3$ could only be explained by a transition between the G-OO/C-AF and C-OO/G-AF phases riding on top of a weak lambda-type anomaly from the ordering of rare earth moments. The dip-like feature is only observable when the entropy change across T^* is reduced by a proper amount of Tb substitution. The dominant G-OO/C-AF phase below T^* , as revealed by X-ray powder diffraction results, suggests that this phase is still favored at the lowest temperatures. The field dependence of $C_p(T)$ data from $DyVO_3$ demonstrates that applied magnetic fields suppress the long range order of Dy^{3+} moments and thus the C-OO/G-AF phase. With increasing magnetic fields, Dy^{3+} ordering is suppressed

but there is a large magnetic polarization at each Dy site as well as a metamagnetic transition. The large polarized Dy^{3+} moments interact with V^{3+} 3d moments, which appears to favor the G-OO/C-AF phase.

CONCLUSIONS

We have investigated the effects of local structure distortions and Dy-V magnetic interactions on the spin and orbital ordering in $\text{Dy}_{1-x}\text{Tb}_x\text{VO}_3$ ($x=0$ and 0.2). Long range magnetic order of Dy^{3+} moments below 12 K introduces a small fraction of the C-OO/G-AF phase in the G-OO/C-AF matrix. External magnetic fields suppress the long range order of Dy^{3+} moments and induce a polarized moment on Dy^{3+} sites which interacts with V^{3+} 3d moments to stabilize the G-OO/C-AF phase. Local structure distortion induced by 20% Tb substitution at the Dy site leads to the coexistence of C-OO/G-AF and G-OO/C-AF phases below T_{CG1} and the volume fraction of each phase is field and temperature dependent. Compared with previous work on the effect of local structure effect on the spin and orbital ordering of $\text{Y}_{1-x}\text{La}_x\text{VO}_3$, $\text{Y}_{1-x}(\text{La}_{0.23}\text{Lu}_{0.77})_x\text{VO}_3$, $\text{Y}_{1-x}\text{Eu}_x\text{VO}_3$, and $\text{Eu}_{1-x}(\text{La}_{0.254}\text{Y}_{0.746})_x\text{VO}_3$, our study suggests that the magnitude of the local stress field around a single foreign atom is another tuning parameter in addition to the average ionic radius and macroscopic size variance.

We noticed that high quality DyVO_3 single crystals crack into pieces after cooling through the first-order transitions. However, with 20% Dy substituted by Tb, the crystals can survive after more than 10 thermal cycles. Together with the fact that Tb substitution could be used to tune the volume fraction of each spin/orbital ordered phase, the doped compositions might provide a rich playground to explore field dependent ferroelectric properties.

ACKNOWLEDGMENTS

JQY thanks H.D. Zhou and J.G. Cheng for helpful discussions and R. J. McQueeney for his support of crystal growth of DyVO_3 at Ames Laboratory. Work at ORNL was supported by the U.S. Department of Energy, Basic Energy Sciences, Materials Sciences and Engineering Division (JQY, MAM, BCS, and DGM) and the Scientific User Facilities Division (HBC). The use of beamline 11-ID-C at the Advanced Photon Source at Argonne National Laboratory was supported by the US Department of Energy, Office of Basic Energy Sciences under Contract No. DE-AC02-06CH11357.

-
- [1] Y. Tokura, and N. Nagaosa, *Science* **288**, 462 (2000).
 - [2] S. Miyasaka, Y. Okimoto, M. Iwama, and Y. Tokura, *Phys. Rev. B* **68**, R100406 (2003).
 - [3] Q. Zhang, K. Singh, C. Simon, L. D. Tung, G. Balakrishnan, and V. Hardy, arXiv:1210.6373.
 - [4] G. R. Blake, T. T. M. Palstra, Y. Ren, A. A. Nugroho, and A. A. Menovsky, *Phys. Rev. B* **65**, 174112 (2002).
 - [5] G. R. Blake, T. T. M. Palstra, Y. Ren, A. A. Nugroho, and A. A. Menovsky, *Phys. Rev. Lett.* **87**, 245501 (2001).
 - [6] Y. Ren, A.A. Nugroho, A. A. Menovsky, J. Strempfer, U. Rtt, F. Iga, T Takabatake, and C. W. Kimball, *Phys. Rev. B* **67**, 014107 (2003).
 - [7] J. B. Goodenough, *Magnetism and the Chemical Bond* (Interscience, New York, 1963)
 - [8] J. Kanamori, *J. Phys. Chem. Solids* **10**, 87 (1959).
 - [9] J.-S. Zhou, J. B. Goodenough, J.-Q. Yan, J.-G. Cheng, K. Matsubayashi, Y. Uwatoko, and Y. Ren. *Phys. Rev. B* **80**, 224422 (2009).
 - [10] J.-S. Zhou, J. B. Goodenough, J.-Q. Yan, and Y. Ren, *Phys. Rev. Lett.* **99**, 156401 (2007).
 - [11] S. Miyasaka, T. Yasue, J. Fujioka, Y. Yamasaki, Y. Okimoto, R. Kumai, T. Arima, and Y. Tokura, *Phys. Rev. Lett.* **99**, 217201 (2007).
 - [12] J. Fujioka, T. Yasue, S. Miyasaka, Y. Yamasaki, T. Arima, H. Sagayama, T. Inami, K. Ishii, and Y. Tokura. *Phys. Rev. B* **82**, 144425 (2010).
 - [13] M. Reehuis, C. Ulrich, K. Prokes, S. Matas, J. Fujioka, S. Miyasaka, Y. Tokura, and B. Keimer. *Phys. Rev. B* **83**, 064404 (2011).
 - [14] J.-Q. Yan, J.-S. Zhou, and J. B. Goodenough, *Phys. Rev. Lett.* **93**, 235901 (2004).
 - [15] B. C. Chakoumakos, H. Cao, F. Ye, A. D. Stoica, M. Poovici, M. Sundaram, W. Zhou, J. S. Kicks, G. W. Lynn, and R. A. Riedel, *J. Appl. Crystallogr.* **44**, 655 (2011).
 - [16] Y. Ren, T. T. M. Palstra, D. I. Khomskii, A. A. Nugroho, A. A. Menovsky, and G. A. Sawatzky. *Phys. Rev. B* **62**, 6577 (2000).
 - [17] J.-Q. Yan, J.-S. Zhou, and J. B. Goodenough. *Phys. Rev. B* **72**, 094412 (2005).
 - [18] J.-Q. Yan, J.-S. Zhou, J. G. Cheng, J. B. Goodenough, Y. Ren, A. Llobet, and R. J. McQueeney. *Phys. Rev. B* **84**, 214405 (2011).
 - [19] J.-Q. Yan, J.-S. Zhou, J. B. Goodenough, Y. Ren, J. G. Cheng, S. Chang, J. Zarestky, O. Garlea, A. Llobet, H. D. Zhou, Y. Sui, W. H. Su, and R. J. McQueeney, *Phys. Rev. Lett.* **99**, 197201 (2007).
 - [20] T. Mizokawa, and A. Fujimori. *Phys. Rev. B* **54**, 5368 (1996).
 - [21] T. Mizokawa, D. I. Khomskii, and G. A. Sawatzky. *Phys. Rev. B* **60**, 7309 (1999).
 - [22] R. Fukuta, S. Miyasaka, K. Hemmi, S. Tajima, D. Kawana, K. Ikeuchi, Y. Yamasaki, A. Nakao, H. Nakao, Y. Murakami, and K. Iwasa. *Phys. Rev. B* **84**, 140409(R) (2011).